

**Influence of the dynamic lattice strain on the transport behavior of oxide heterojunctions**

J. Wang, F. X. Hu, L. Chen, Y. Y. Zhao, H. X. Lu, J. R. Sun, and B. G. Shen

Citation: [Applied Physics Letters](#) **102**, 022423 (2013); doi: 10.1063/1.4788731

View online: <http://dx.doi.org/10.1063/1.4788731>

View Table of Contents: <http://scitation.aip.org/content/aip/journal/apl/102/2?ver=pdfcov>

Published by the [AIP Publishing](#)

---



## Re-register for Table of Content Alerts

Create a profile.



Sign up today!





## Influence of the dynamic lattice strain on the transport behavior of oxide heterojunctions

J. Wang,<sup>a)</sup> F. X. Hu, L. Chen, Y. Y. Zhao, H. X. Lu, J. R. Sun, and B. G. Shen  
*State Key Laboratory of Magnetism, Institute of Physics, Chinese Academy of Sciences,  
 Beijing 100190, People's Republic of China*

(Received 16 August 2012; accepted 4 January 2013; published online 18 January 2013)

All-perovskite oxide heterojunctions composed of electron-doped titanate  $\text{La}_x\text{Sr}_{1-x}\text{TiO}_3$  ( $x = 0.1, 0.15$ ) and hole-doped manganite  $\text{La}_{0.67}\text{Ca}_{0.33}\text{MnO}_3$  films were fabricated on piezoelectric substrate of (001)- $0.7\text{Pb}(\text{Mg}_{1/3}\text{Nb}_{2/3})\text{O}_3$ - $0.3\text{PbTiO}_3$  (PMN-PT). Taking advantage of the excellent converse piezoelectric effect of PMN-PT, we investigated the influence of the dynamic lattice strain on transport properties of the heterojunctions by applying external bias electric fields on the PMN-PT substrate. Photovoltaic experiments were carried out to characterize the interfacial barrier of the heterojunction. A linear reduction in the barrier height was observed with the increase of the bias field applied on PMN-PT. The value of the barrier height reduces from  $\sim 1.55$  ( $\sim 1.30$ ) to 1.02 (1.08) eV as the bias field increases from 0 to 12 kV/cm for the junction of  $\text{La}_{0.10}\text{Sr}_{0.9}\text{TiO}_3/\text{La}_{0.67}\text{Ca}_{0.33}\text{MnO}_3$  ( $\text{La}_{0.15}\text{Sr}_{0.85}\text{TiO}_3/\text{La}_{0.67}\text{Ca}_{0.33}\text{MnO}_3$ ). The observed dependency of barrier height on external field can be ascribed to the increasing release of trapped carriers by strain modulation, which results in a suppression of the depletion layer and increases the opportunity for electron tunneling across the depletion area. © 2013 American Institute of Physics. [<http://dx.doi.org/10.1063/1.4788731>]

Manganite-based heterostructures provide a pathway to create attractive functional devices and combinations of fascinating physical phenomena.<sup>1–3</sup> Some researches have shown that manganite junctions exhibit many distinctive features including magnetic field-dependent rectifying property,<sup>4</sup> bias-dependent magnetoresistance,<sup>5</sup> and temperature-dependent photovoltaic effect,<sup>6</sup> which are absent in conventional junctions. As well established, the properties of the junction are mainly determined by the interfacial barrier (IB), which is strongly influenced by interface states including structural and electronic states. Much effort has been put into tuning the rectifying behaviors of the junction by adjusting interface, for the purpose of either fundamental research or practical application. As well documented, the biaxial strain due to lattice mismatch between film and substrate plays a very important role in controlling the electrical transport and magnetic properties of manganite thin films because of the strong electron-lattice coupling.<sup>7–12</sup> Indeed, Lü *et al.* have found that the IB can be tuned by chemical stress (hole contents) for  $\text{La}_{1-x}\text{Ca}_x\text{MnO}_3/\text{SrTiO}_3:\text{Nb}$  junctions.<sup>13</sup> Moreover, the tensile stress in the manganite film, imposed by substrate, was also found to have an obvious impact on the height of the IB.<sup>14</sup> Therefore, if effectively controlling stress near the interface of the manganite-based junction, one could obtain functional devices. However, such modulations through carrier doping or thickness variation are badly controllable because of the randomness inhomogeneous and bad repeatability of the strain relaxation progresses. In addition, the substrate induced static lattice strain is always accompanied by many other parameters, such as defects, microstructure, compositions etc. These accompanying factors would obstruct the investigations of the pure strain effect on properties of junctions.

Recently, a linear and reversible tuning of the lattice strain and, hence, the electronic properties of the thin films by applying an electric field have been reported in perovskite thin films epitaxially grown on ferroelectric relaxor  $(1-x)\text{Pb}(\text{Mg}_{1/3}\text{Nb}_{2/3})\text{O}_3$ - $x\text{PbTiO}_3$ .<sup>9–12,15,16</sup> Taking advantage of such dynamically strain tuning method, one could expect to modify, *reliably and reversibly*, the interface state of the manganite-based junction such as carrier concentration and IB by varying the Jahn-Teller distortion and preferred occupancy of particular orbital.<sup>17</sup> In this Letter, we report the evolution of the rectifying and photoelectric properties with the dynamic strain modification.

The commercial (001)-oriented  $0.7\text{Pb}(\text{Mg}_{1/3}\text{Nb}_{2/3})\text{O}_3$ - $0.3\text{PbTiO}_3$  (PMN-PT) single crystal was chosen as the substrate due to its perovskite cubic structure ( $a_{\text{PMN-PT}} = 4.017 \text{ \AA}$ ) and outstanding ferroelectric and converse piezoelectric effects (remnant polarization  $P_r \sim 22.9 \mu\text{C}/\text{cm}^2$  and coercivity field  $E_c \sim 2.8 \text{ kV}/\text{cm}$ ), which makes it a nice platform in investigating the impact of substrate induced tensile strain on the transport behaviors of manganite-based junction dynamically.<sup>9–12</sup> We selected  $\text{La}_{0.67}\text{Ca}_{0.33}\text{MnO}_3$  ( $\text{LCMO}, a_{\text{LCMO,bulk}} = 3.868 \text{ \AA}$ ) and 15% (and 10%) La-doped  $\text{SrTiO}_3$  ( $\text{La}_x\text{Sr}_{1-x}\text{TiO}_3$  ( $x = 0.10, 0.15$ )) ( $\text{LSTO}, a_{\text{LSTO,bulk}} = 3.905 \text{ \AA}$ ) to compose a heterojunction. The former is a *p*-type degenerated semiconductor while the latter is *n*-type with different carrier concentration due to different doping level.<sup>18</sup> The samples thus obtained will be denoted as LSTO(15)/LCMO and LSTO(10)/LCMO, respectively. The LSTO-LCMO/PMN-PT junction was fabricated by successively growing LCMO and LSTO films with the thickness of  $t = 30, 150 \text{ nm}$  on the (001)-PMN-PT substrate using pulsed laser deposition technique. The temperature of the substrate was kept at  $670^\circ\text{C}$  and the oxygen pressure at 100 Pa and 50 Pa during the deposition of LCMO and LSTO films, respectively. The crystalline structures of the samples were determined by means of x-ray diffraction (XRD)

<sup>a)</sup> Author to whom correspondence should be addressed. Electronic mail: wangjing@iphy.ac.cn.

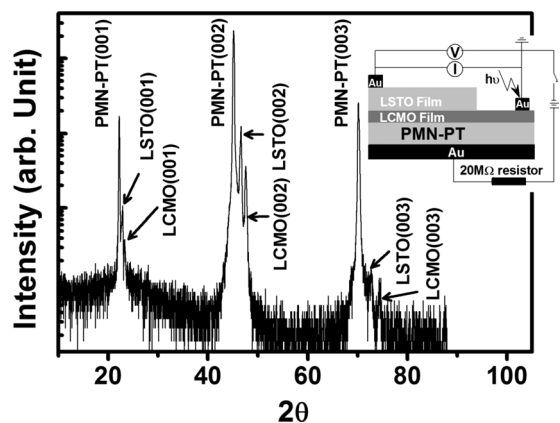


FIG. 1. X-ray diffraction patterns of the LSTO(10)/LCMO heterojunction. The inset shows a schematic diagram of the junction structure and the circuit for electrical measurements.

using Cu-K $\alpha$  radiation. Several Au pads were deposited respectively on LCMO, LSTO, and the bottom of PMN-PT as electrodes (junction area =  $1 \times 1 \text{ mm}^2$ ). The dynamic and reversible strain modulation of LCMO film was achieved by applying a bias field up to 12 kV/cm across the PMN-PT substrate (for protection, a 20 M $\Omega$  resistor is presented in the circuit, see inset of Fig. 1). The resistance of the PMN-PT, measured using a Keithley 6517 A electrometer, was  $\sim 10 \text{ G}\Omega$ , and a negligible small leakage current was observed (less than 15 nA under a 12 kV/cm electric field). The inset of Fig. 1 shows the schematic junction structure and the circuit for electrical measurements. Lasers with wavelengths between 532 and 780 nm were used in the photovoltaic experiments. The spot size of the laser is  $\sim 1 \text{ mm}$  in diameter. The current-voltage ( $J$ - $V$ ) characteristics of the junction, as well as photocurrent ( $I_p$ ) yielded by laser illumination, were measured at ambient temperature by a Keithley 2611 SourceMeter.

Figure 1 shows typical  $\theta$ - $2\theta$  XRD patterns of the LSTO(10)/LCMO junction, which indicates the single pseudocubic phase and high crystallinity for both layers. It was found that the reflections of LSTO and LCMO, with degressive intensities, appear in sequence at the right side of the PMN-PT reflection, in accordance with the relation of the lattice parameters  $a_{\text{PMN-PT}} > a_{\text{LSTO,bulk}} > a_{\text{LCMO,bulk}}$  and the stack sequence of the junction LSTO-LCMO on the PMN-PT substrate. The out-of-plane lattice parameter  $c$  for LSTO and LCMO were determined to be 3.897 and 3.820  $\text{\AA}$  from respective positions of (002) reflection peak, indicating that both films undergo compressive out-of-plane strains

( $\epsilon_{zz} = (c_{\text{film}} - c_{\text{bulk}})/c_{\text{bulk}} = -0.21\%$  for LSTO,  $-1.23\%$  for LCMO). Corresponding in-plane tensile strains were calculated as 0.35% and 1.57% by Poisson relation  $\epsilon_{xx} = -(1 - \nu)/2\nu\epsilon_{zz}$  using  $\nu = 0.232$  (Ref. 19) and 0.282.<sup>20</sup> The obtained lower in-plane strain of LCMO compared to the nominal mismatch between LCMO and PMN-PT ( $\sim 3.85\%$ ) reveals that the strain of LCMO film has undergone a partial relaxation. For the film of LSTO, a rough analysis of the relaxation state can be made by estimating the in-plane parameter of the strained LCMO taking into account the in-plane biaxial strain. It was found that in-plane strain (0.35%) of the present LSTO film is lower than the nominal mismatch between LSTO and the strained LCMO ( $\sim 0.58\%$ ), indicating that the film of LSTO also undergoes a partial relaxation. Biegalski *et al.* has measured the in-plane diffraction of the bilayer STO-LSMO on PMN-PT (Ref. 21) using four-circle x-ray diffractometer. The in-plane lattice parameters determined from diffractions reveal that the film of STO (having a similar lattice parameter compared to LSTO) exhibit a partial relaxation which is in accordance with our results. It is noted that the film of LSTO(10) shows little strain, which should be ascribed to the relative small mismatch between LSTO and the strained LCMO film. The relaxation of the LSTO film probably also contributes to the small strain. Similar phenomena were also observed in the sample of LSTO(15)/LCMO, which has out-of-plane lattice parameters of 3.899/3.821  $\text{\AA}$ . The surface morphology of the PMN-PT substrate, LCMO film, and LSTO/LCMO was investigated by atomic force microscopy. The surface roughness RMS was found to be 1.35, 1.51, and 1.81 nm for PMN-PT substrate, LCMO film, and LSTO(10)/LCMO, respectively. The small increase of roughness for both LCMO and LSTO/LCMO indicates the films are well grown and the interface between LCMO and LSTO and that between LCMO and the PMN-PT substrate are satisfactory.

Transport measurements of the LCMO layer were made by using a superconducting quantum interference device (SQUID) magnetometer. Fig. 2(a) shows temperature dependent resistance for the LCMO layer under different magnetic field and bias fields. First, it was found that the insulator-metal transition temperature  $T_{\text{IM}}$  for the film moves from the bulk of  $\sim 250 \text{ K}$  (Ref. 22) to  $\sim 207 \text{ K}$  due to the static tensile strain, coinciding with previous reports.<sup>15,23</sup> Such reduction in transition temperature is due to the decrease of the in-plane transfer integral for the ferromagnetic double-exchange coupling through enlarged in-plane Mn-O-Mn bond. One also noted that a magnetic field of 5 T shifts the transition temperature upwards by  $\sim 45 \text{ K}$  and reduce the resistance considerably. On

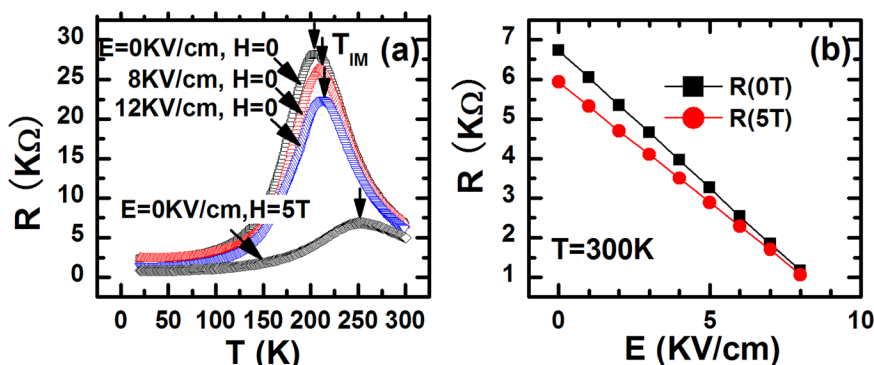


FIG. 2. (a) Temperature dependence of the resistance for the LCMO film when the PMN-PT substrate is under a bias field of 0, 8, and 12 kV/cm, respectively. The results under 5 T magnetic field (0 kV/cm) were also plotted; (b) Resistance of the LCMO film at 300 K as a function of the electric bias field applied to the PMN-PT substrate under 0 T and 5 T.

the other hand, while a bias field,  $E$ , was applied on the PMN-PT substrate, the resistance of the LCMO film (without any magnetic field applied) decreases over a wide temperature range as shown in Fig. 2(a). The decrease in resistance is particularly pronounced near  $T_{IM}$  where the resistance decreases by  $\sim 21\%$  for  $E=8$  kV/cm and  $\sim 35\%$  for  $E=12$  kV/cm. Moreover,  $T_{IM}$  shifts towards high temperature by  $\sim 3$  K and  $\sim 6$  K for  $E=8$  kV/cm and 12 kV/cm, respectively. We attributed such reductions in the resistance and increases of  $T_{IM}$  to the strain effect induced by the bias field on the PMN-PT substrate.<sup>10,15</sup> Previous researches<sup>10,15</sup> have revealed that the bias-field-induced compressive strain in the PMN-PT substrate could impose in-plane compressive strains on the LCMO film and thus a decrease of the Jahn-Teller distortion, thereby resulting in delocalization of charge carriers. Meanwhile, the bias-field-induced compressive strain can also cause a decrease in the in-plane Mn-O-Mn bond length and an enhancement in the hopping of carriers and double exchange (DE) interaction, resulting in a reduction in resistivity and an increase in  $T_{IM}$ .

Furthermore, we also measured the resistance in the LCMO film as a function of the electric bias field  $E$  applied to the PMN-PT substrate at 300 K, and the results are shown in Fig. 2(b). One could immediately find that the resistance at 300 K decreases linearly with increasing bias field. Considering that the bias-field-induced strain is linearly dependent on the bias field,<sup>15,21</sup> this result implies that the change in resistance, and probably, the delocalized charge carriers due to bias-field-induced strain is proportional to the modulation of the in-plane strain. It is reasonable to anticipate that the external bias field could be also used to modulate the interfacial barrier and transport properties of the heterojunction composed of LCMO and LSTO.

The current density-voltage ( $J$ - $V$ ) relations of both junctions under selected bias fields, measured at ambient temper-

ature, were presented in Figs. 3(a) and 3(b). One can distinguish obvious rectifying characteristic, noting the obvious asymmetric  $J$ - $V$  curves. It was found that an increase of bias field causes the curve shifts up under forward voltage biases (directing from LCMO to LSTO), which indicates the decrease in the junction resistance due to the external bias field on PMN-PT. In Figs. 3(c) and 3(d), the forward junction resistance  $R_{\text{junction}}$  at various forward voltage biases  $V_{\text{bias}}$ , defined as  $R_{\text{junction}}(V_{\text{bias}}) = V_{\text{bias}}/J_{\text{interface}}$ , was plotted as a function of the bias field. One can find that the junction resistance, in both samples, decreases linearly with the external bias field,  $E$ , at all  $V_{\text{bias}}$ . This intriguing behavior suggests that the concentration of effective holes near the interface of LCMO film varies with the dynamic strain variation from substrate. It has been reported that the piezoelectric lattice strain of the PMN-PT substrate, resulting from the external electric field, could transfer to the manganite film on it.<sup>15,16</sup> In present system, a bias field of 12 kV/cm could induce a reduction of  $\sim 0.11\%$  in in-plane strain for 30 nm LCMO film.<sup>15</sup> As well known, the reduction in in-plane strain would weaken Jahn-Teller distortion and release trapped charge, leading to a dramatic enhancement of the hole concentration in LCMO film.

Xie *et al.*<sup>24</sup> has reported that the depletion layer of the junction LCMO-STON will be suppressed if the released hole concentration increases. It is reasonable to infer that similar suppression of the depletion layer would appear in present LSTO/LCMO heterojunctions due to the enhancement of carrier concentrations. As a result, the junction resistance decreases with the external bias field. Moreover, one could expect that the suppression of the depletion layer would result in a reduction of the effective barrier height of the junction.

It is known that the technique of photovoltaic effect can be used to investigate the junction in its equilibrium state and avoid the adverse effect related to an external voltage.<sup>25</sup>

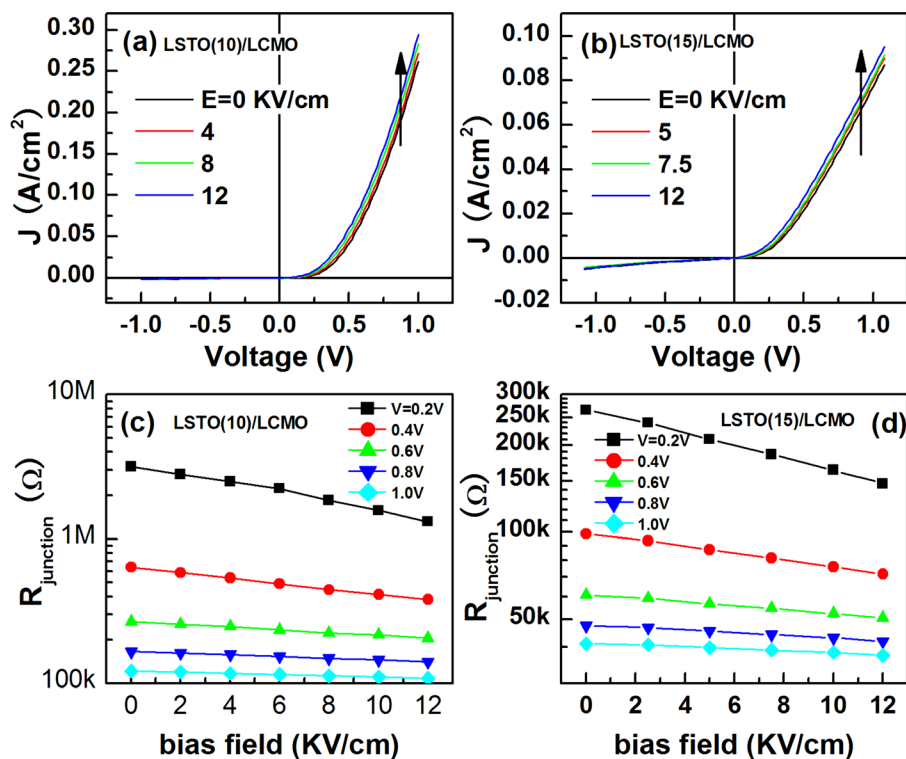


FIG. 3. Current-voltage characteristics under selected bias fields measured at room temperature for (a) LSTO(10)/LCMO and (b) LSTO(15)/LCMO junctions. (c), (d) The junction resistance as a function of bias field under different forward voltage for corresponding samples.

To investigate the influence of the dynamic strain on the interfacial barrier, we acquired photocurrent of the junction under various bias fields,  $I_p$ , yielded by laser (wavelength from 532 to 780 nm) illumination at ambient temperature. It was found that the photocurrent, for a fixed wavelength, shows a remarkable dependence on the bias field. Figs. 4(a) and 4(b) present the photocurrents produced by the light of 532 nm under a bias field of 0 and 12 kV/cm for both junctions. Sudden jumps in photocurrent of both junctions are observed when the light is on and off (indicated by arrows in Figs. 4(a) and 4(b)), suggesting a fast response to light illumination. Moreover, one can find that the photocurrent in both junctions increases as the bias field on PMN-PT increases. The typical value for the junction LSTO(10)/LCMO under a laser of 532 nm is  $\sim 2.6$  nA/mW, for a bias field of 0, and  $\sim 10.4$  nA/mW, for 12 kV/cm. This feature indicates a change in the barrier height with the bias field, i.e., the strain variation in the film.

As well known, the information about the IB can be extracted from internal photoemission spectra. According to Fowler's theory,<sup>26</sup> the quantum efficiency  $R$  of the photoemission, which is proportional to the photocurrent yielded by each photon, is a simple function of photon energy:  $R \propto (h\nu - \Phi_b)^2$  if  $E_F \gg |h\nu - \Phi_b| \gg 3k_B T$ , where  $h\nu$  is the photon energy and  $\Phi_b$  the interfacial barrier height. A direct calculation

shows that the depletion layer mainly develops in LSTO. As a result, LSTO-LCMO can be well approximated by a Schottky junction, and the Fowler equation could be used safely. Figures 4(c) and 4(d) show the square root of the quantum efficiency as a function of photon energy for both LSTO(10)/LCMO and LSTO(15)/LCMO junctions under various external bias fields. At first glance, the  $R^{1/2}$ - $h\nu$  slope increases with the increase of bias field, which might be a consequence of the reduced annihilation of the extra carriers. Moreover, one could also find that the x-axis intercept of the  $R^{1/2}$ - $h\nu$  curve shifts to low energies while the bias field increases, indicating the IB decreases while the in-plane strain decreases. The specific  $\Phi_b$  under different bias fields, deduced from Fowler equation, are illustrated in the inset of Figs. 4(e) and 4(f). It is worthwhile to note that the LSTO(15)/LCMO exhibits a lower barrier than LSTO(10)/LCMO, which is probably due to a relative thin depletion layer resulting from the high carrier concentration of LSTO(15).

A clear suppression of the IB by external bias field was found in both junctions (see Figs. 4(e) and 4(f)). Biegalsk *et al.*<sup>21</sup> has found that the change in the in-plane strain of the film with the external electric field applied on the PMN-PT substrate is identical to that in the substrate strain. Taking this

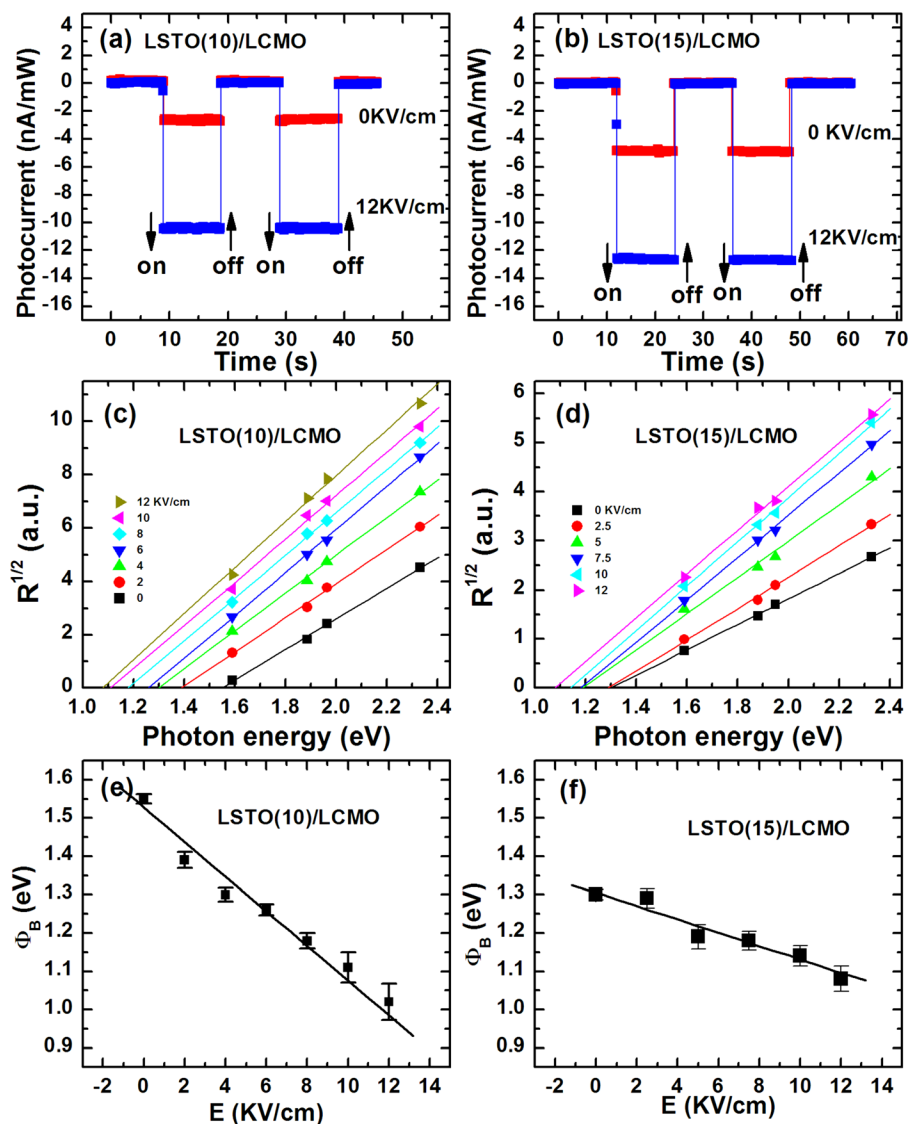


FIG. 4. Photocurrents produced by the light of 532 nm under a bias field of 0 and 12 kV/cm for (a) LSTO(10)/LCMO and (b) LSTO(15)/LCMO junctions. Arrows signify the positions of light on and off; (c), (d) Square-root quantum efficiency as a function of photon energy for corresponding junctions under different external bias fields (strain state). Solid lines are fitting results; (e), (f) the IB height, extracted from photovoltaic effect, as a function of the external bias field for corresponding junctions.

into account, one may conclude that the present result demonstrates the impact of the reduction in the tensile strain of LCMO on the IB of the junction. As discussed above and revealed by previous reports,<sup>10–12</sup> the further relaxation of the LCMO film (the reduction of the tensile strain) caused by the substrate strain due to the converse piezoelectric effect would cause an enhancement of the hole concentration in LCMO, resulting in a suppression of depletion layer. Such suppression of depletion layer would increase opportunities for electron tunneling across the depletion area and results in a reduction in the effective barrier height. Thus, the variation of the hole concentration near the partial-relaxed LCMO/LSTO interface and the interfacial barrier could be regarded as a function of the PMN-PT substrate strain since their direct cause, the in-plane strain, is a uniform response of the PMN-PT substrate strain induced by external electric fields. Furthermore, one could find, interestingly, that the modulation of the IB is also nearly linear in the investigated range of  $E$ . Considering that the nearly linear relationship between reversible strain and  $E$ ,<sup>15</sup> a linear dependence of the IB on strain is reasonable. To provide an intuitive estimation of the influence of the strain on interfacial barrier, we calculate the gauge factor ( $d\Phi_b/d\varepsilon_{xx}$ ), defined as the ratio of the change in barrier height and the in-plane strain variation. Gauge factor values of  $\sim 492$  and  $190$  for junctions of LSTO(10)/LCMO and LSTO(15)/LCMO are obtained from the data of photovoltaic experiments, respectively, taking into account that the in-plane strain variations in the films are similar to the substrate strain changes  $\sim 0.11\%$  for  $E = 12\text{ kV/cm}$ .<sup>15,16</sup> The clear discrepancy in obtained gauge factors for two junctions might relate to the different Fermi level and energy band structure due to the different doping content of La in LSTO layers.

So far, our discussion on the strain effect on the barrier is focused on the LCMO films. The in-plane dynamic strain of the substrate upon bias field may also transfer to the LSTO ( $\text{La}_x\text{Sr}_{1-x}\text{TiO}_3$  ( $x = 0.10, 0.15$ )) film,<sup>21</sup> resulting in a reduction of in-plane tensile strain in LSTO. However, the strain effect on LSTO is not clear at the moment. A similar investigation<sup>27</sup> on the tensile strain effect for  $\text{SrTiO}_3$  (STO) film indicated that the in-plane tensile strain would lower the electron effective mass of the  $\text{SrTiO}_3$  film, resulting in an increase of electron mobility. We notice that LSTO and STO have similar lattice and parameters. For a preliminary discussion, we assume similar effect may also occur in the LSTO film. The bias field-induced strain would reduce the in-plane strain in LSTO and enhance the electron effective mass, especially at the interface with LCMO, hence reducing the electron mobility. However, the possible change of electron mobility in LSTO upon bias field does not imply any change of carrier concentration, thus its influence on the barrier of LCMO/LSTO junction should not be significant. In other words, the change of electron mobility may only affect the carrier's moving speed, and should not affect the height of barrier. Thus the strain change of LSTO film due to the bias field may not play a dominant role in modifying the barrier height, and the change of the interfacial potential barrier should mainly come from the contribution of LCMO film.

In conclusion, the influence of strain modulation on the transport properties of manganite-based junction LSTO-LCMO/PMN-PT has been investigated by the converse

piezoelectric effect in (001) PMN-PT. It was found that the IB of the junction, extracted from photovoltaic effect, has a nearly linear dependence on the external bias field applied on PMN-PT. Such interesting correlation between the interfacial barrier and the external bias field can be mainly ascribed to the stimulation of trapped carriers due to the tensile strain reduction in the LCMO film caused by external bias field.

This work was supported by National Basic Research program of China (973 program), the National Natural Science Foundation of China, Hi-Tech Research and Development program of China, and the Key Research Program of the Chinese Academy of Sciences.

<sup>1</sup>M. Sugiura, K. Urugou, M. Noda, M. Tachiki, and T. Kobayashi, *Jpn. J. Appl. Phys., Part 1* **38**, 2675 (1999).

<sup>2</sup>H. Tanaka, J. Zhang, and T. Kawai, *Phys. Rev. Lett.* **88**, 027204 (2002); J. Zhang, H. Tanaka, and T. Kawai, *Appl. Phys. Lett.* **80**, 4378 (2002).

<sup>3</sup>F. X. Hu, J. Gao, J. R. Sun, and B. G. Shen, *Appl. Phys. Lett.* **83**, 1869 (2003).

<sup>4</sup>D. J. Wang, J. R. Sun, Y. W. Xie, W. M. Lü, S. Liang, T. Y. Zhao, and B. G. Shen, *Appl. Phys. Lett.* **91**, 062503 (2007).

<sup>5</sup>Y. W. Xie, J. R. Sun, Y. N. Han, and B. G. Shen, *Appl. Phys. Lett.* **91**, 262515 (2007).

<sup>6</sup>J. R. Sun, B. G. Shen, Z. G. Sheng, and Y. P. Sun, *Appl. Phys. Lett.* **85**, 3375 (2004).

<sup>7</sup>J. Zhang, H. Tanaka, T. Kanki, J. H. Choi, and T. Kawai, *Phys. Rev. B* **64**, 184404 (2001).

<sup>8</sup>T. Kanki, T. Yanagida, B. Vilquin, H. Tanaka, and T. Kawai, *Phys. Rev. B* **71**, 012403 (2005).

<sup>9</sup>A. D. Rata, A. Herklotz, K. Nenkov, L. Schultz, and K. Dörr, *Phys. Rev. Lett.* **100**, 076401 (2008).

<sup>10</sup>R. K. Zheng, Y. Wang, J. Wang, K. S. Wong, H. L. W. Chan, C. L. Choy, and H. S. Luo, *Phys. Rev. B* **74**, 094427 (2006).

<sup>11</sup>J. Wang, F. X. Hu, L. Chen, J. R. Sun, and B. G. Shen, *J. Appl. Phys.* **109**, 07D715 (2011); L. Chen, F. X. Hu, J. Wang, J. Shen, J. R. Sun, B. G. Shen, J. H. Yin, and L. Q. Pan, *ibid.* **109**, 07D713 (2011).

<sup>12</sup>J. Wang, F. X. Hu, R. W. Li, J. R. Sun, and B. G. Shen, *Appl. Phys. Lett.* **96**, 052501 (2010).

<sup>13</sup>W. M. Lü, J. R. Sun, D. J. Wang, Y. W. Xie, S. Liang, Y. Z. Chen, and B. G. Shen, *Appl. Phys. Lett.* **93**, 212502 (2008).

<sup>14</sup>W. M. Lü, A. D. Wei, J. R. Sun, Y. Z. Chen, and B. G. Shen, *Appl. Phys. Lett.* **94**, 082506 (2009).

<sup>15</sup>C. Thiele, K. Dörr, S. Fähler, and L. Schultz, *Appl. Phys. Lett.* **87**, 262502(2005); C. Thiele, K. Dörr, O. Bilani, J. Rödel, and L. Schultz, *Phys. Rev. B* **75**, 054408 (2007).

<sup>16</sup>A. A. Levin, A. I. Pommrich, T. Weißbach, D. C. Meyer, and O. Bilani-Zeneli, *J. Appl. Phys.* **103**, 054102 (2008).

<sup>17</sup>M. Huijben, L. W. Martin, Y.-H. Chu, M. B. Holcomb, P. Yu, G. Rijnders, D. H. A. Blank, and R. Ramesh, *Phys. Rev. B* **78**, 094413 (2008); Y. Tokura and N. Nagaosa, *Science* **288**, 462 (2000).

<sup>18</sup>S. Liang, D. J. Wang, J. R. Sun, and B. G. Shen, *Solid State Commun.* **148**, 386 (2008).

<sup>19</sup>H. Ledbetter, M. Lei, and S. Kim, *Phase Trans.* **23**, 61 (1990).

<sup>20</sup>J. J. U. Buch, G. Lalitha, T. K. Pathak, N. H. Vasoya, V. K. Lakhani, P. V. Reddy, K. Ravi, and K. B. Modi, *J. Phys. D: Appl. Phys.* **41**, 025406 (2008).

<sup>21</sup>M. D. Biegalski, K. Dörr, D. H. Kim, and H. M. Christen, *Appl. Phys. Lett.* **96**, 151905 (2010).

<sup>22</sup>P. Schiffer, A. P. Ramirez, W. Bao, and S.-W. Cheong, *Phys. Rev. Lett.* **75**, 3336 (1995).

<sup>23</sup>Z. G. Sheng, J. Gao, and Y. P. Sun, *Phys. Rev. B* **79**, 174437 (2009).

<sup>24</sup>Y. W. Xie, J. R. Sun, J. Wang, S. Liang, W. M. Lü, and B. G. Shen, *Appl. Phys. Lett.* **90**, 192903 (2007).

<sup>25</sup>Y. Hikita, Y. Kozuka, T. Susaki, H. Takagi, and H. Y. Hwang, *Appl. Phys. Lett.* **90**, 143507(2007); Y. Hikita, M. Nishikawa, T. Yajima, and H. Y. Hwang, *Phys. Rev. B* **79**, 073101 (2009).

<sup>26</sup>R. H. Fowler, *Phys. Rev.* **38**, 45 (1931).

<sup>27</sup>A. Janotti, D. Steiauf, and C. G. Van de Walle, *Phys. Rev. B* **84**, 201304(R) (2011).